Probing gluon spin-momentum correlations in transversely polarized protons through midrapidity isolated direct photons in $p^{\uparrow}+p$ collisions at $\sqrt{s} = 200$ GeV

PHENIX Collaboration Author List (Brant will insert later)

(Dated: October 14, 2020)

Spin-momentum correlations in hadronic collisions offer a glimpse into a three-dimensional picture of proton structure. The transverse single-spin asymmetry for midrapidity isolated direct photons in $p^{\uparrow} + p$ collisions at $\sqrt{s} = 200$ GeV with the PHENIX detector at the Relativistic Heavy Ion Collider (RHIC) is measured. Since direct photons are produced from the hard scattering and do not interact via the strong force, these results are a clean probe of initial-state spin-momentum correlations inside the proton and are in particular sensitive to gluon interference effects within the proton. This is the first time direct photons have been used as a probe of spin-momentum correlations at RHIC. The uncertainties on the results are a fifty-fold improvement with respect to those of the one prior measurement for the same observable, from the Fermilab E704 experiment. These results constrain gluon spin-momentum correlations in transversely polarized protons.

***** page break for PRL word count *****

Unlike lepton-hadron scattering measurements, proton-proton collisions are sensitive to gluon scattering at leading order. Direct photons are produced *directly* in the hard scattering of partons and because they do not interact via the strong force are a phenomenologically clean probe of the structure of the proton. At large transverse momentum, direct photons are produced at leading order via the quantum chromodynamics (QCD) 2-to-2 hard scattering subprocesses quark-gluon Compton scattering ($g+q \to \gamma+q$) and quark-antiquark annihilation ($\bar{q}+q \to \gamma+g$). Compton scattering dominates at midrapidity [1] because the proton is being probed at moderate longitudinal momentum fraction, x, where gluons dominate the proton. Thus midrapidity direct photon measurements are a clean probe of gluon structure within the proton.

Transverse single-spin asymmetries (TSSAs) in hadronic collisions are sensitive to various spin-momentum correlations, i.e. correlations between the directions of the spin and momentum of partons and/or hadrons involved in a scattering event. In collisions between one transversely polarized proton and one unpolarized proton, the TSSA describes the azimuthal-angular dependence of particle production relative to the transverse polarization direction. TSSAs have been measured as large as 40% in forward charged pion production [2–5] and significantly nonzero asymmetries have been measured with transverse momentum up to $p_T \sim 7$ GeV/c [6, 7]. In this context, p_T serves as a proxy for a hard momentum scale Q that is well into the perturbative regime of QCD. Next-to-leading-order (NLO) purely perturbative QCD calculations which only include effects from high energy parton scattering predict that these asymmetries should be small and fall off as m_q/Q [8] where m_q is the bare mass of the quark. Thus in order to explain these large TSSAs, they must be considered in the context of the dynamics present in proton-proton collisions that cannot be calculated perturbatively, namely those describing proton structure and/or the process of hadronization.

One approach toward explaining the large measured TSSAs is through transverse-momentum-dependent (TMD) functions. As the name implies, these TMD functions depend on the soft-scale parton transverse momentum, k_T, in addition to the partonic longitudinal momentum fraction, x, and the hard scattering energy, Q, where $k_T \ll Q$. TMD functions can be directly extracted from measurements that are sensitive to two momentum scales, such as Semi-Inclusive Deep Inelastic Scattering (SIDIS) where the angle and energy of the scattered electron can be used to directly measure the hard scale, Q, and the transverse momentum of the measured hadron can be used as a proxy for the soft-scale, k_T. The Sivers function is a parton distribution function (PDF) that describes the structure of the transversely polarized proton and correlates the transverse spin of the proton and k_T of the parton within it [9], analogous to the hyperfine structure in atomic physics. The quark Sivers function has been extracted through polarized SIDIS measurements, but the gluon Sivers function has remained comparatively less constrained because SIDIS is not sensitive to gluons at leading order. The direct photon TSSA in proton-proton collisions has been shown to be sensitive to the gluon Sivers function [10], but the k_T moment of TMD functions must be taken in order to apply them to the single-scale inclusive TSSAs measured in proton-proton collisions.

Twist-3 correlation functions are another approach toward describing TSSAs. Unlike TMD functions, collinear twist-3 correlation functions depend only on a single scale, the hard scale Q. Twist-3 functions describe spin-momentum correlations generated by the quantum mechanical interference between scattering off of one parton versus scattering off two. There are two different types: the quark-gluon-quark (qgq) correlation functions and the trigluon (ggg) correlation function. In the context of proton structure, qgq correlation functions describe the quantum mechanical interference between scattering off of a single quark in the proton versus scattering off of a quark of the same flavor and the same momentum fraction plus an additional gluon. Analogously, the trigluon correlation describes the quantum mechanical interference between scattering off of one gluon in the proton versus scattering off of two. Collinear twist-3 functions have been shown to be related to the k_T moment of TMD functions [11, 12]. For example the Qiu-Sterman function is a qgq correlation function for the polarized proton [13, 14] that is related to the k_T moment of the Sivers TMD PDF. The Qiu-Sterman function has also been extracted from fits to inclusive TSSAs in proton-proton collisions [15, 16] and the forward direct photon TSSA has been shown to be dominated by this Qiu-Sterman function [17].

The trigluon correlation function in the polarized proton has been estimated through studying inclusive heavy flavor hadron TSSA measurements [18], but it remains relatively unconstrained compared to the qgq functions due to statistical limitations [19]. Midrapidity jet TSSAs that also probe gluon dynamics inside of the proton have been measured to be consistent with zero [20, 21]. While jets are not sensitive to the details of hadronization, unlike direct photons they are still sensitive to potential final-state color interactions. The direct photon TSSA has been shown to be sensitive to the trigluon correlation function [22]. The fact that both TMD and collinear twist-3 functions are nonzero reflects that scattering partons do in fact interact with the color fields present inside the proton, which goes beyond traditional assumptions present in hadronic collision studies.

The only previously published direct photon TSSA measurement came from the E704 experiment at Fermilab in 1995 using a 200 GeV/c polarized proton beam on an unpolarized proton target ($\sqrt{s} = 19.4$ GeV). It was found to be consistent with zero to within 20% for $2.5 < p_T^\gamma < 3.1$ GeV/c [23]. The PHENIX results presented in this Letter measure photons with $p_T^\gamma > 5$ GeV/c and have total uncertainties up to a factor of 50 smaller than the E704 measurements. This measurement will constrain multigluon correlations in transversely polarized protons.

This measurement was performed using $p^{\uparrow}+p$ collisions at $\sqrt{s} = 200$ GeV for $|\eta| < 0.35$ with the PHENIX experiment. The data set was collected in 2015 and corresponds to an integrated luminosity of approximately 60 pb^{-1}. Direct photons were reconstructed using similar techniques to a previously published direct photon cross section result at $\sqrt{s} = 200$ GeV [24]. The asymmetry was measured with transversely polarized proton beams at RHIC where the clockwise beam had an average polarization of 0.58 ± 0.02 and the average polarization of the counter-clockwise beam was 0.60 ± 0.02 [25]. The polarization direction changes bunch-to-bunch such that two statistically independent asymmetries can be measured with the same particle yields. This is achieved by sorting the yields by the polarization direction in one beam, effectively averaging over the polarization in the other beam. This allows for two independent measurements that serve as a cross check and are averaged together to calculate the final asymmetry.

The PHENIX central detector consists of two nearly-back-to-back arms each covering $\Delta\phi = \pi/2$ in azimuth and $|\eta| < 0.35$ in pseudorapidity. Photons are identified through clusters in the electromagnetic calorimeter (EMCal), which has two detector arms: the west and the east. The west arm is composed of four sectors of sampling lead-scintillator (PbSc) calorimeters with granularity $\delta\phi \times \delta\eta = 0.011 \times 0.011$ and the east arm consists of two more PbSc sectors along with two sectors of Cherenkov lead-glass (PbGl) calorimeters with granularity $\delta\phi \times \delta\eta = 0.008 \times 0.008$ [26]. The Beam-Beam Counters (BBC) are far-forward arrays of quartz Cherenkov radiators that cover the full azimuth and $3.0 < |\eta| < 3.9$ in pseudorapidity [27]. They measure the z-vertex position, for which a 30 cm vertex cut around the nominal collision point is applied. The minimum bias trigger fires on crossings where at least one charged particle is measured in each arm of the BBC. Events with high p_T photons are selected through an EMCal based high energy photon trigger that is taken in coincidence with this minimum bias trigger. The PHENIX central tracking system uses pad chambers and a drift chamber to measure the position of charged particle tracks [28].

All photons are required to pass certain cuts including a shower shape cut that reduces the contributions from hadron clusters. A time-of-flight cut of $|TOF| < 5$ ns suppresses the contributions from EMCal noise, where the timing of the cluster is measured by the EMCal and the time zero reference of the event provided by the BBC. A charged track veto cut eliminates clusters that geometrically match with a charged track and uses the track position measured directly in front of the EMCal. This cut reduces the background from electrons as well as charged hadrons that were not eliminated by the shower shape cut.

Direct photon candidates are also required to pass tagging cuts that reduce the hadronic decay background by eliminating photons that are tagged as coming from either $\pi^0 \to \gamma\gamma$ or $\eta \to \gamma\gamma$ decays. The candidate direct photon is matched with a partner photon in the same event and same EMCal arm which is required to pass a minimum energy cut of 0.5 GeV. A photon is considered tagged as coming from a $\pi^0 \to \gamma\gamma$ ($\eta \to \gamma\gamma$) decay if it is matched into a photon pair with invariant mass $105 < M_{\gamma\gamma} < 165$ MeV/c^2 ($480 < M_{\gamma\gamma} < 620$ MeV/c^2), which corresponds roughly to a $\pm 2\sigma$ window around the observed π^0 and η peaks.

Additionally, direct photon candidates are required to pass an isolation cut, which further reduces the contribution of decay photons [24]. Ref. [1] estimates that the contribution of NLO fragmentation photons to the isolated direct photon sample is less than 15%. The photon isolation cut requires that the sum of the particles' energy surrounding the photon in a cone of radius $r = \sqrt{(\Delta\eta)^2 + (\Delta\phi)^2} < 0.4$ radians be less than 10% of the candidate photon's energy: $E_{cone} < E_\gamma \cdot 10\%$. In order to be included in the cone sum energy, E_{cone}, an EMCal cluster is required to have a minimum energy of 0.15 GeV and a charged track needs to have a minimum momentum of 0.2 GeV/c. To provide a more inclusive sample of the particles surrounding the photon, the clusters and tracks that are included in the E_{cone} sum are only required to pass a minimum set of quality cuts. The charged track veto cut is still used to ensure charged particles are not double counted by the energy that they deposit in the EMCal. The shower shape cut is not applied to EMCal clusters to ensure that neutral hadrons and charged hadrons that were not reconstructed as charged tracks can still contribute to E_{cone}.

This asymmetry measurement used similar techniques to previously published PHENIX TSSAs which include Refs. [18] and [29]. The TSSA is determined using the "relative luminosity formula"

$$A_N = \frac{1}{P\ \langle\cos(\phi)\rangle} \frac{N^{\uparrow} - \mathcal{R}N^{\downarrow}}{N^{\uparrow} + \mathcal{R}N^{\downarrow}}, \tag{1}$$

where $\mathcal{R} = \mathcal{L}^{\uparrow}/\mathcal{L}^{\downarrow}$ is the relative luminosity of collisions for when the beam was polarized up versus down. P is the average polarization of the beam and $\langle\cos(\phi)\rangle$ is the acceptance factor which accounts for the azimuthal coverage of each detector arm. In Eq. (1), N refers to the particle yield and the up ($\uparrow$) or down ($\downarrow$) arrow superscripts refer to the direction of the beam polarization. The asymmetries are calculated separately for each arm of the detector and averaged together for the final result weighted by the statistical uncertainty.

The main source of direct photon background comes from decay photons that were not eliminated by the tagging cut because their partner photon was not measured. This can occur because the partner photon was out of acceptance, hit a dead area of the detector, or did not pass the minimum energy cut. The measured TSSA of the isolated direct photon candidate sample, A_N^{iso}, is corrected for the background

$$A_N^{dir} = \frac{A_N^{iso} - r_{\pi^0} A_N^{iso,\pi^0} - r_\eta A_N^{iso,\eta}}{1 - r_{\pi^0} - r_\eta} \qquad (2)$$

by subtracting the background asymmetries from isolated π^0 photons, A_N^{iso,π^0}, and isolated η photons, $A_N^{iso,\eta}$. In Eq. (2), r_{π^0} and r_η are the fractional contribution of photons from π^0 and η decays, respectively. Both the midrapidity π^0 and η TSSAs have been measured to be consistent with zero to high statistical precision [29], and after confirming that their isolated asymmetries are also consistent with zero, both A_N^{iso,π^0} and $A_N^{iso,\eta}$ are set to zero in Eq. (2). In other words, the direct photon background is treated as a dilution. A systematic uncertainty due to the assumption that the isolated π^0 and η asymmetries are zero is assigned by propagating through Eq. (2) the statistical uncertainty of the inclusive midrapidity π^0 and η TSSAs integrated over photon p_T. This systematic uncertainty dominates the total systematic uncertainty for all p_T bins.

Calculating the contribution of decay photons where the second photon was missed is performed by taking the ratio of measured photon yields: $N_{tag}^{iso,h}/N^{iso}$. Here N^{iso} is the isolated direct photon candidate sample and $N_{tag}^{iso,h}$ is the number of photons that were tagged as coming from either a π^0 or η decay which pass the photon pair isolation cut, $E_{cone} - E_{partner} < E_\gamma \cdot 10\%$, which subtracts off the energy of the partner photon, $E_{partner}$. Photons that pass this photon pair isolation cut would have been included in the isolated direct photon candidate sample had their partner photon not been detected. Simulations are used to calculate how to convert from the number of tagged decay photons to the number of decay photons where the partner photon was missed. The background fraction for photons from π^0 and η meson decays is calculated separately to account for their differences in particle production and decay kinematics.

$$r_h = R_h \frac{N_{tag}^{iso,h}}{N^{iso}} \qquad (3)$$

The one-miss ratio, R_h, is calculated with single particle Monte Carlo and takes the ratio of the number of photons for which only one of the simulated decay photons was reconstructed to the number of photons in which both decay photons were reconstructed [24]. These simulations include the geometry, resolution, and configuration of the dead areas of the EMCal and use the previously measured π^0 [30] and η [31] cross sections. The background fractions for photons from π^0 (η) decays are plotted in Figure 1 and are systematically larger in the east arm versus the west due to the PbGl sectors having slightly more dead area compared to the PbSc sectors.

A similar method to Eq. (3) is used to find the contribution of merged π^0 decay photons, where a high energy π^0 decays into a photon pair with such a small decay angle that it is resolved as a single cluster in the EMCal.

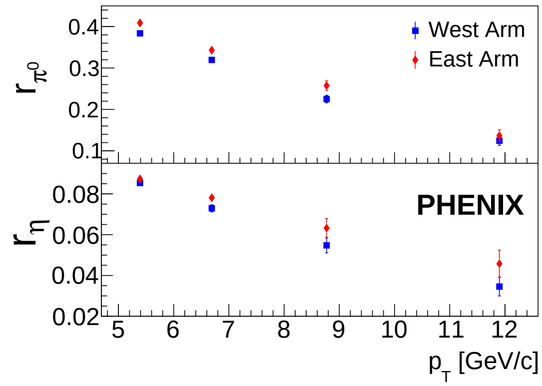

FIG. 1. The fractional contribution of photons from π^0 (top) and η (bottom) decays to the isolated direct candidate photon sample.

The contribution from merged photon clusters was found to be less than 0.2% and the contribution from merged η decays was confirmed to be negligible. This background fraction due to π^0 merging is added to the uncertainty on the background fraction from Eq. (3) which is propagated through the background correction formula as a systematic uncertainty.

An additional systematic study is performed by calculating the asymmetry with the "square root formula"

$$A_N = \frac{1}{P\,\langle\cos(\phi)\rangle} \frac{\sqrt{N_L^\uparrow N_R^\downarrow} - \sqrt{N_L^\downarrow N_R^\uparrow}}{\sqrt{N_L^\uparrow N_R^\downarrow} + \sqrt{N_L^\downarrow N_R^\uparrow}}, \qquad (4)$$

where the L and R subscripts refer to yields to the left and to the right of the polarized-beam-going direction, respectively. This result is verified to be consistent with the relative luminosity formula results from Eq. (1) and the differences between these results are assigned as an additional systematic uncertainty due to possible variations in detector performance and beam conditions. Bunch shuffling is a systematic study that is used to confirm that the variations present in the data are consistent with what is expected by statistical variation. This is performed by randomizing the bunch-by-bunch polarization directions of the beam. No additional systematic effects were found using this study.

The result for A_N of isolated direct photons at midrapidity in $p^\uparrow$+p collisions at $\sqrt{s} = 200$ GeV is shown in Figure 2 where the shaded grey bands represent the systematic uncertainty and the bars represent the statistical uncertainty. The measurement is consistent with zero to within 1% across the entire p_T range. Figure 2 also shows predictions from collinear twist-3 correlation functions. The green curve shows the contribution of qgq correlation functions to the direct photon asymmetry which is calculated using functions that were published in Ref. [17] that are integrated over the $|\eta| < 0.35$ pseudorapidity range of the PHENIX central arms. This calculation includes contributions from the qgq correlation functions

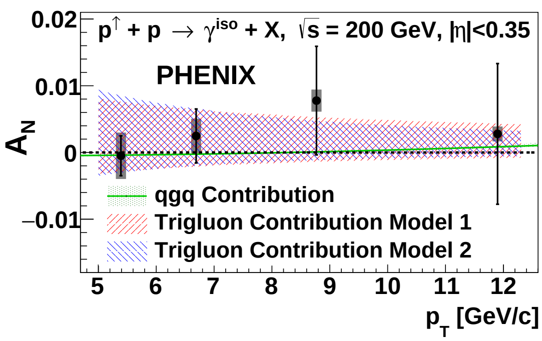

FIG. 2. Transverse single-spin asymmetry of isolated direct photons measured at midrapidity $|\eta| < 0.35$ in $p^{\uparrow}+p$ collisions at $\sqrt{s} = 200$ GeV. An additional scale uncertainty of 3.4% due to the polarization uncertainty is not shown.

TABLE I. The measured A_N of isolated direct photons in $p^{\uparrow}+p$ collisions at $\sqrt{s}$ =200 GeV as a function of p_T. An additional scale uncertainty of 3.4% due to the polarization uncertainty is not included.

$\langle p_T \rangle$[GeV/c]	A_N	$\sigma_{\rm stat}$	$\sigma_{\rm syst}$
5.39	-0.000492	0.00299	0.00341
6.69	0.00247	0.00404	0.00252
8.77	0.00777	0.00814	0.00159
11.88	0.00278	0.0105	0.00106

present in both the polarized and unpolarized proton, including the Qiu-Sterman function which is extracted from a global fit in Ref. [16]. The error band plotted with the green curve in Figure 2 includes uncertainties propagated from fits to data, but does not include uncertainties associated with assuming functional forms.

Because the qgq correlation functions' contribution to the midrapidity direct photon TSSA is predicted to be small, this measurement can provide a clean extraction of the ggg function. The predicted ranges for the trigluon correlation function's contribution to the direct photon asymmetry are also plotted in Figure 2. They use results that were published in Ref. [19] and were reevaluated as a function of photon p_T for pseudorapidity $\eta = 0$. Models 1 and 2 assume different functional forms for the trigluon correlation function, which are designed to study the sensitivity of the TSSA at small momentum fractions. The bands plotted in Figure 2 are a result of maximizing and minimizing the direct photon TSSA and do not include uncertainties associated with assuming the functional forms. Nevertheless, this figure clearly shows that this measurement has the statistical precision at low p_T to constrain the trigluon correlation function.

The TSSA of midrapidity isolated direct photons was measured by the PHENIX experiment to be consistent with zero in the presented p_T range, with uncertainties as low as 0.4% in the lowest p_T bins. This is the first time direct photons have been used to probe transversely polarized proton collisions at RHIC and first measurement of this TSSA in almost 30 years with significantly higher precision and p_T reach. Direct photons are a clean probe of proton structure with no contributions from final-state QCD effects and at midrapidity are particularly sensitive to gluon dynamics. This measurement will constrain gluon spin-momentum correlations in the transversely polarized proton, which is a step toward creating a more three-dimensional picture of proton structure.

***** page break for PRL word count <3.5 pages <7 columns**

[1] A. Adare *et al.* (PHENIX), "High p_T direct photon and π^0 triggered azimuthal jet correlations and measurement of k_T for isolated direct photons in $p+p$ collisions at $\sqrt{s}$ = 200 GeV," Phys. Rev. D **82**, 072001 (2010), arXiv:1006.1347 [hep-ex].

[2] R. D. Klem, J. E. Bowers, H. W. Courant, H. Kagan, M. L. Marshak, E. A. Peterson, K. Ruddick, W. H. Dragoset, and J. B. Roberts, "Measurement of Asymmetries of Inclusive Pion Production in Proton Proton Interactions at 6-GeV/c and 11.8-GeV/c," Phys. Rev. Lett. **36**, 929–931 (1976).

[3] D. L. Adams *et al.* (FNAL-E704 Collaboration), "Analyzing power in inclusive π^+ and π^- production at high x_F with a 200-GeV polarized proton beam," Phys. Lett. **B264**, 462–466 (1991).

[4] C.E. Allgower *et al.*, "Measurement of analyzing powers of π^+ and π^- produced on a hydrogen and a carbon target with a 22-GeV/c incident polarized proton beam," Phys. Rev. D **65**, 092008 (2002).

[5] I. Arsene *et al.* (BRAHMS Collaboration), "Single Transverse Spin Asymmetries of Identified Charged Hadrons in Polarized $p+p$ Collisions at $\sqrt{s} = 62.4$ GeV," Phys. Rev. Lett. **101**, 042001 (2008).

[6] S. Heppelmann, "Large p_T Forward Transverse Single Spin Asymmetries of π^0 Mesons at $\sqrt{s}$=200 and 500 GeV from STAR," POS **DIS2013**, 240 (2013).

[7] Christopher Dilks (STAR Collaboration), "Measurement of Transverse Single Spin Asymmetries in π^0 Production from $p^\uparrow + p$ and $p^\uparrow + A$ Collisions at STAR," PoS **DIS2016**, 212 (2016), arXiv:1805.08875 [hep-ex].

[8] G. L. Kane, J. Pumplin, and W. Repko, "Transverse Quark Polarization in Large p_T Reactions, e^+e^- Jets, and Leptoproduction: A Test of QCD," Phys. Rev. Lett. **41**, 1689 (1978).

[9] D. W. Sivers, "Single Spin Production Asymmetries from the Hard Scattering of Point-Like Constituents," Phys. Rev. **D41**, 83 (1990).

[10] Rohini M. Godbole, Abhiram Kaushik, Anuradha Misra, and Siddhesh Padval, "Probing the Gluon Sivers Function through direct photon production at RHIC," Phys. Rev. D **99**, 014003 (2019), arXiv:1810.07113 [hep-ph].

[11] Daniel Boer, P.J. Mulders, and F. Pijlman, "Universality of T odd effects in single spin and azimuthal asymmetries," Nucl. Phys. B **667**, 201–241 (2003), arXiv:hep-ph/0303034.

[12] Xiangdong Ji, Jian-Wei Qiu, Werner Vogelsang, and Feng Yuan, "A Unified picture for single transverse-spin asymmetries in hard processes," Phys. Rev. Lett. **97**, 082002 (2006), arXiv:hep-ph/0602239.

[13] Jian-wei Qiu and George F. Sterman, "Single transverse spin asymmetries in direct photon production," Nucl. Phys. B **378**, 52–78 (1992).

[14] Jian-wei Qiu and George F. Sterman, "Single transverse spin asymmetries in hadronic pion production," Phys. Rev. D **59**, 014004 (1999), arXiv:hep-ph/9806356.

[15] Koichi Kanazawa, Yuji Koike, Andreas Metz, and Daniel Pitonyak, "Towards an explanation of transverse single-spin asymmetries in proton-proton collisions: the role of fragmentation in collinear factorization," Phys. Rev. D **89**, 111501 (2014), arXiv:1404.1033 [hep-ph].

[16] Justin Cammarota, Leonard Gamberg, Zhong-Bo Kang, Joshua A. Miller, Daniel Pitonyak, Alexei Prokudin, Ted C. Rogers, and Nobuo Sato (Jefferson Lab Angular Momentum), "Origin of single transverse-spin asymmetries in high-energy collisions," Phys. Rev. D **102**, 054002 (2020), arXiv:2002.08384 [hep-ph].

[17] K. Kanazawa, Y. Koike, A. Metz, and D. Pitonyak, "Transverse single-spin asymmetries in $p^\uparrow p \to \gamma X$ from quark-gluon-quark correlations in the proton," Phys. Rev. D **91**, 014013 (2015), arXiv:1410.3448 [hep-ph].

[18] C. Aidala *et al.* (PHENIX), "Cross section and transverse single-spin asymmetry of muons from open heavy-flavor decays in polarized p+p collisions at $\sqrt{s}$ = 200 GeV," Phys. Rev. D **95**, 112001 (2017), arXiv:1703.09333 [hep-ex].

[19] Yuji Koike and Shinsuke Yoshida, "Probing the three-gluon correlation functions by the single spin asymmetry in $p^\uparrow p \to DX$," Phys. Rev. D **84**, 014026 (2011), arXiv:1104.3943 [hep-ph].

[20] L. Adamczyk *et al.* (STAR), "Longitudinal and transverse spin asymmetries for inclusive jet production at mid-rapidity in polarized $p+p$ collisions at $\sqrt{s}$ = 200 GeV," Phys. Rev. D **86**, 032006 (2012), arXiv:1205.2735 [nucl-ex].

[21] J. Adam *et al.* (STAR), "Longitudinal double-spin asymmetry for inclusive jet and dijet production in pp collisions at $\sqrt{s}$ = 510 GeV," Phys. Rev. D **100**, 052005 (2019), arXiv:1906.02740 [hep-ex].

[22] Yuji Koike and Shinsuke Yoshida, "Three-gluon contribution to the single spin asymmetry in Drell-Yan and direct-photon processes," Phys. Rev. D **85**, 034030 (2012), arXiv:1112.1161 [hep-ph].

[23] D.L. Adams *et al.* (E704), "Measurement of single spin asymmetry for direct photon production in p p collisions at 200-GeV/c," Phys. Lett. B **345**, 569–575 (1995).

[24] A. Adare *et al.* (PHENIX), "Direct-Photon Production in $p+p$ Collisions at $\sqrt{s}$ = 200 GeV at Midrapidity," Phys. Rev. D **86**, 072008 (2012), arXiv:1205.5533 [hep-ex].

[25] W. D. Schmidke *et al.* (The RHIC Polarimetry Group), "RHIC polarization for Runs 9–17," https://technotes.bnl.gov/Home/ViewTechNote/209057 (2018).

[26] L. Aphecetche *et al.* (PHENIX), "PHENIX calorimeter," Nucl. Instrum. Meth. **A499**, 521–536 (2003).

[27] M. Allen *et al.*, "PHENIX inner detectors," Nucl. Instrum. Meth. A **499**, 549–559 (2003).

[28] K. Adcox *et al.* (PHENIX), "PHENIX central arm tracking detectors," Nucl. Instrum. Meth. A **499**, 489–507 (2003).

[29] C. Aidala *et al.*, "Transverse single-spin asymmetries of midrapidity π^0 and η mesons in $p+p$ collisions at $\sqrt{s}$ = 200 GeV," (2020), arXiv:TBD [hep-ph].

[30] A. Adare *et al.* (PHENIX), "Inclusive cross-section and double helicity asymmetry for π^0 production in $p+p$ collisions at $\sqrt{s}$ = 200 GeV: Implications for the polarized gluon distribution in the proton," Phys. Rev. D **76**, 051106 (2007), arXiv:0704.3599 [hep-ex].

[31] A. Adare *et al.* (PHENIX), "Cross section and double helicity asymmetry for η mesons and their comparison to neutral pion production in p+p collisions at $\sqrt{(s)} = 200$ GeV," Phys. Rev. D **83**, 032001 (2011), arXiv:1009.6224

[hep-ex].